Desalination and Water Treatment
www.deswater.com

doi: 10.1080/19443994.2015.1011702

57 (2016) 6702–6711
March

Taylor & Francis
Taylor & Francis Group

Degradation of refractory organics in chemical industry wastewater using iron (II) Schiff base complex as homogeneous catalyst in Fenton-like oxidation

S. Pavithra[a], A. Madonna[b], S. Swarnalatha[a], K. Mohan Das[b,*], A.B. Mandal[a], G. Sekaran[a,*]

[a]*Environmental Technology Division, Council of Scientific & Industrial Research (CSIR) - Central Leather Research Institute (CLRI), Adyar, Chennai 600 020, India, Tel. +91 44 24437132; emails: pavijeni28@gmail.com (S. Pavithra), swarnavinayak2009@gmail.com (S. Swarnalatha), Tel. +91 44 24910897; email: abmandal@hotmail.com (A.B. Mandal), Tel. +91 44 24452491; Fax: +91 44 24912150; email: sekaransabari@gmail.com (G. Sekaran)*
[b]*Department of Chemistry, Madras Christian College, Chennai 600 059, India, Tel. +91 44 24437132; email: madonaanziojohn@gmail.com (A. Madonna), Tel. +91 9566296310; email: mohan1@gmail.com (K. Mohan Das)*

Received 17 March 2014; Accepted 20 January 2015

ABSTRACT

Degradation of biorefractory compounds in wastewater generated from a chemical industry using iron (II) Schiff base complex as homogeneous catalyst. The complex of iron (II) Schiff base was derived from o-vanillin and allyl thio urea. The ligand and the complex were characterized using FT-IR, UV–Visible, fluorescence spectroscopy, SEM–EDX, and elemental composition. The optimized conditions for degradation were carried out with different time, pH, temperature, dosage of the complex, and H_2O_2. The chemical oxygen demand was reduced from 3,360 to 1,200 mg/L (64.3% reduction) at the optimized conditions such as pH, temperature, iron (II) Schiff base complex, and H_2O_2. The degradation of chemicals in wastewater was confirmed with the ^{13}C-NMR, ^{1}H-NMR, high performance liquid chromatography (HPLC), and fluorescence spectroscopy.

Keywords: Iron (II) Schiff base complex; Azomethane; Fenton oxidation; Tannery wastewater; Refractory organics

1. Introduction

Generation of wastewater has become an integral activity in most of the industrial manufacturing practices. Being an economically viable process, biological treatment has been recognized as a versatile option to remove/reduce part of the organic load. High organic load, refractory organics (derived from wastewater or from the micro-organism), and presence of toxic compounds impair the efficiency of biological treatment processes. The most effective technologies to remove organic pollutants from aqueous solutions are known as advanced oxidation processes (AOPs). The common aspect among the AOPs is the generation of hydroxyl radical, which possess high oxidation potential (2.83 V). Hydroxyl radicals are extremely unstable with high reactivity [1]. The generation of hydroxyl radicals can be achieved by a variety of physico-chemical reactions such as ozone/UV, hydrogen peroxide, Fenton oxidation, photo-Fenton, and titanium dioxide/hydrogen peroxide/solar radiation. Fenton reaction has been widely used in the practice as a source of hydroxyl radicals for oxidation of organics in wastewater [2]. The kinetics of Fenton oxidation of

*Corresponding authors.

organics reactions is first order with respect to hydroxyl radical concentration and the concentration of pollutant [3]. Among the AOPs, the oxidation of organics in wastewater using Fenton reagent (ferrous ion and hydrogen peroxide) at acidic pH 3.5 has been considered as one of the essential operating conditions in wastewater treatment [4].

The generation of hydroxyl radicals by Fenton reagent is represented as in Eq. (1):

$$Fe^{2+} + H_2O_2 \rightarrow Fe^{3+} + OH^- + OH^{\cdot} \quad (1)$$

The ferric ion produced can react with H_2O_2 to regenerate Fe^{2+} along with hydroperoxy radical Eq. (2) [4].

$$Fe^{3+} + H_2O_2 \rightarrow Fe^{2+} + HO_2^{\cdot} + H^+ \quad (2)$$

Patra et al. [5] developed iron containing core–shell nanoparticles and $Al_2O_3@Fe_2O_3$ supported mesoporous core–shell nanoparticles, and were used as a Fenton catalyst in the presence of H_2O_2 as oxidant. Fe over HY zeolite has been used for the degradation of polyvinyl alcohol [6]. The immobilization of Fe ions on clays, bentonite, and laponite for the oxidation of azo dye orange II has also been reported [7]. Karthikeyan et al. used iron (III) oxide doped nanoporous carbon [8] as the Fenton reagent for the treatment of wastewater.

There is a considerable opportunities for the formation of ferric hydroxide from ferric ion and hydroxide ion as per the Eq. (1) in conventional Fenton oxidation. The formation of ferric hydroxide sludge may be considered as the short comings of conventional Fenton oxidation process. The ferric hydroxide sludge serves as a heterogeneous catalyst to decompose hydrogen peroxide causing higher consumption of Fenton reagent [9]. The post Fenton oxidation processes demand the adjustment of pH of the wastewater to the neutral condition resulting in high total dissolved solids and high sludge formation. Thus, there has been a constant research on the development of an effective Fenton oxidation process to oxidize the organics in wastewater at neutral pH.

Schiff bases are the iron-based complexes, having substance stability (Stability constant -8.21×10^{10}) at neutral pH [10]. Schiff bases have been widely employed in many fields such as biological, inorganic, and analytical chemistry [11]. Thus, an iron–Schiff base complex was considered to carry out Fenton oxidation at neutral pH in the present investigation.

Hence, the focal theme of the present investigation is to oxidize the refractory organics present in chemical industry wastewater using iron (II) Schiff base complex as the heterogeneous catalyst at neutral pH.

2. Materials and methods

2.1. Materials

Ethanol, allyl thio urea, and o-vanilline were purchased from Merck (India) and used as received. The wastewater used in the present investigation was collected from a common effluent treatment plant, treating the wastewater discharged from the chemicals manufacturing industrial cluster in Gujarat, India. Over half of these are chemical units, manufacturing dyes, paints, fertilizers, pharmaceuticals, industrial chemicals, pulp and paper, and pesticides [12]. Out of total capacity of the wastewater generated, 58% arises from dyes and dyes' intermediates, 19% from drugs and pharmaceuticals, and 5% from inorganic chemicals manufacturing industries [12]. The organic compounds found in the wastewater are derivatives of phenol, aniline, and benzene. The major compounds are nitrophenol, aniline, naphthalene, and benzyl alcohol.

2.2. Preparation of Schiff base ligand

The Schiff base ligand was prepared using the method adopted by Rizwana and Lakshmi [13]. An ethanolic solution of allylthiourea (0.351 g, 3 mmol) was added to an ethanolic solution of o-vanillin (0.456 g, 3 mmol) at 1:1 M ratio and few drops of sodium hydroxide solution (0.05 N) were added subsequently. The mixture was then stirred for 4 h in a magnetic stirrer (340 RPM) until the solution turned yellow in color. The solvent was evaporated over a water bath at 28°C to get the Schiff base ligand as yellow oil. It was washed with ethanol and dried at room temperature.

2.3. Synthesis of iron (II) Schiff base complex

$FeSO_4 \cdot 7H_2O$ (3 mmol) and sodium per chlorate (3 mmol) were added to the prepared Schiff base ligand and the mixture was stirred using a magnetic stirrer for 4 h at constant temperature. The solid product obtained was filtered, washed with ethanol, and dried at room temperature to get iron (II) Schiff base complex (Fe-ligand).

2.4. Characterization of iron (II) Schiff base complex

UV–Visible spectrophotometer (Shimadzu model UV-3600), which offers an absorbance in wavelength

ranging from 200–800 nm with path length of 10 mm was used.

A Fourier transform infrared spectrometer (Perkin–Elmer) was used for the investigation of the surface functional groups. The samples were mixed with KBr of spectroscopic grade and made into pellets at a pressure of about 1 MPa. The pellets of dimensions: diameter 10 mm and thickness 1 mm. The samples were scanned in the spectral range of wavenumber 4,000–400 cm^{-1}.

Scanning electron microscopy (SEM) images and Energy-dispersive X-ray spectroscopy (EDX) patterns were collected on a Jeol JSM-6390.

The total iron concentration in the complex was determined by using an atomic absorption spectrophotometer (Shimadzu AA 6650) after digesting the complex following standard method of wastewater.

2.5. Characterization of wastewaters

The pH, ORP, chemical oxygen demand (COD), and biochemical oxygen demand (BOD), and total organic content (TOC) of wastewater samples were analyzed in accordance with standard methods of wastewater.

2.6. Fenton oxidation of organics in wastewater at neutral pH using iron (II) Schiff complex

The wastewater samples were screened to remove floating solids. The pH of the wastewater was adjusted to 7.0 using 0.1 N sulfuric acid. The wastewater was treated with different concentrations of iron (II) Schiff base complex and hydrogen peroxide to achieve the maximum degradation. The contents were agitated using compressed air of volume 3 L min^{-1}. The temperature of the reaction was maintained using a thermostat control. Optimization studies were carried out by varying pH (3.5, 4.5, 5.5, 7.0, and 8.5), temperature (30, 40, 50, 60, and 70°C), mass of iron complex (0.05, 0.1, 0.15, 0.2, and 0.25 g), H_2O_2 concentration (4, 8, 16, 24, and 32 mmol) and time (1, 2, 3, 4, 5, 6, and 7 h). The reduction in COD was used as the online parameter for optimization of the process.

2.6.1. Confirmation of degradation of compounds in wastewater

Proton and 13C-NMR spectra were recorded using Bruker Avance 111 500 MHZ(AV500) MUH Nuclei Solution NMR. For initial sample deuterated DMSO-D6 was used as the solvent, whereas $CDCl_3$ was used for treated sample. Pre-column derivatized samples were measured with Waters (Milford, MA) HPLC unit, which consisted of waters 600 multisolvent delivery system, and acetonitrile was used as a solvent. Fluorescence spectra of wastewater samples before and after Fenton oxidation were recorded using fluorescence spectroscopy (Cary ellipse).

3. Results and discussion

3.1. Characterization of Schiff–iron complex

3.1.1. Elemental composition of Schiff–iron complex

The data on elemental analysis of the Ligand and Fe-ligand are presented in Table 1. The percentage of iron present in the iron Schiff base complex was 7.93% as determined with AAS spectroscopy.

3.1.2. UV–Visible spectrum of Schiff–iron complex

The electronic absorption spectra of Ligand and Fe-ligand were recorded in the wavelength range of 200–800 nm using ethanol as solvent. The electronic spectrum of free Schiff base showed absorption bands at λ 310, 352 nm which are characteristic $\pi \rightarrow \pi^*$ and $n \rightarrow \pi^*$ transitions (Fig. 1(a)). In the Schiff–iron complex, the band at 352 nm is shifted to a longer wave length (366 nm) with increasing intensity. This shift may be attributed to the donation of lone pair electrons of nitrogen of Schiff base to Fe(II). Fig. 1(b) shows Fe-ligand complex exhibited strong absorption in the wavelength range 251–259 nm and 308–373 nm [13]. The broad intense and resolved bands were around 308–366 nm. The high intensity band at λ 310 nm is of ligand origin assignable to intra ligand $n \rightarrow \pi^*$ and $\pi \rightarrow \pi^*$ transitions.

3.1.3. Fluorescence spectroscopy

Fluorescence emission spectrometry is the device in which emission is scanned in the range of wavelengths for a fixed excitation wavelength.

The excitation spectra of Schiff base ligand displayed the maximum intensity excitation wavelength at λ 306 nm. Upon excitation at 306 nm (within the charge transfer envelope) in ligand shows weak emission band with maximum at λ 451 nm (Fig. 2(a)). The emission observed in these ligands can be tentatively assigned to the intraligand, which is related to the energy gap between the $\pi \rightarrow \pi^*$ molecular orbital of the π-conjugation in the ligand system.

The Fe(II) Schiff complex containing the ligand displayed the maximum excitation wavelength at λ 282 nm and its corresponding emission at λ 310 nm

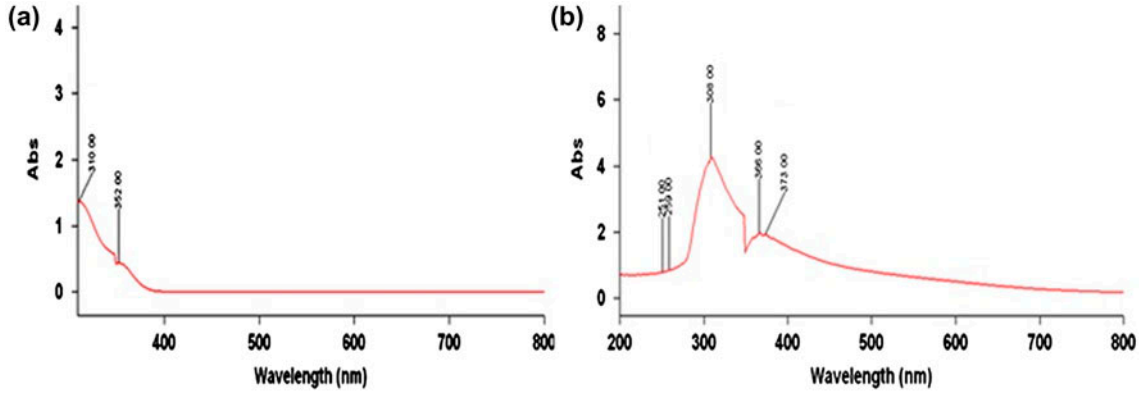

Fig. 1. (a) UV–Visible spectra for Schiff base complex and (b) UV–Visible spectra for iron–Schiff base complex.

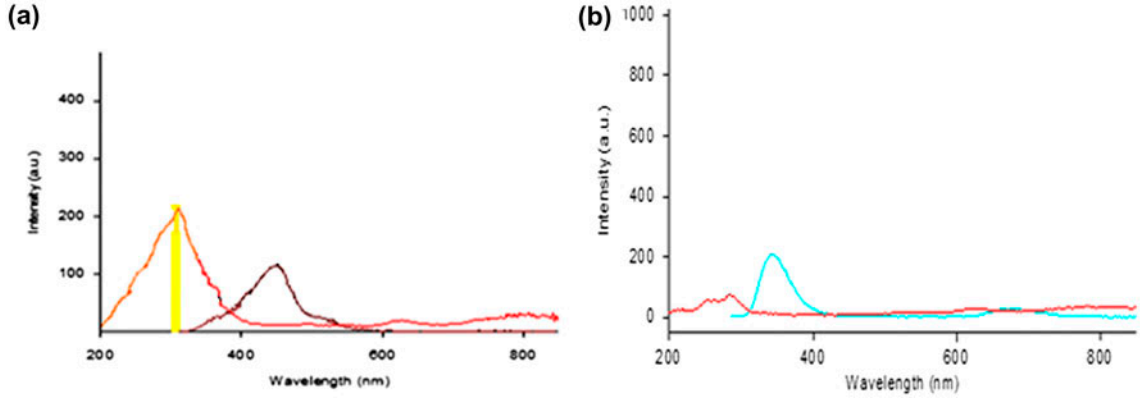

Fig. 2. (a) Fluorescence spectra for Schiff base complex and (b) Fluorescence spectra for iron–Schiff base complex.

(Fig. 2(b)). Fluorescent emission is related to the energy gap between $\pi \rightarrow \pi^*$ molecular orbital of the π-conjugation of the ligand system. The fluorescence emission observed in the complex at room temperature is ascribed to intraligand $\pi \rightarrow \pi^*$ transition mixed with metal-ligand charge transfer transitions and are red shifted by lesser than 60 nm as compared to the corresponding free ligand. It has been observed that metal ions can enhance the fluorescence emission of nitrogen. The complexation with metal ions effectively increased the rigidity of the ligands and reduced the loss of energy via radiation less thermal vibrational decay [13].

3.1.4. SEM/EDX

Morphology and chemical component of the complex is studied by the SEM–EDX. The SEM image (Fig. 3) illustrates the iron crystals embedded in the matrix of Schiff complex. The EDX image suggests that the complex contained the redox couple Fe^{2+}/Fe^{3+}. The presence of Fe^{2+}/Fe^{3+} redox couple may be employed for the oxidation of organics in wastewater.

3.1.5. FT-IR

Table 2 shows the FT-IR frequencies corresponding to various stretching present in the ligand and in the complex. The FT-IR spectrum of Schiff's complex shows the peak at 3,055.4 cm^{-1} may be assigned to –NH stretching of secondary amine and the peak at 3,440 cm^{-1} may be attributed to hydroxyl group of water molecule (may be due to the absorbed water molecule). The stretching at 1,620.11 cm^{-1} confirms the presence of C=N bonding of the ligand. Formation of the Schiff base ligand was confirmed by the appearance of a band at 1,620 cm^{-1}, which can be attributed to azomethine group [13]. The peak at 728 cm^{-1} is correlated with C–S stretching of the complex.

The FT-IR spectrum of Fe(II)–Schiff base complex shows the peak at 1,614.77 cm^{-1}, denotes the lower shift of 1,620.11 cm^{-1} peak present in Schiff's complex.

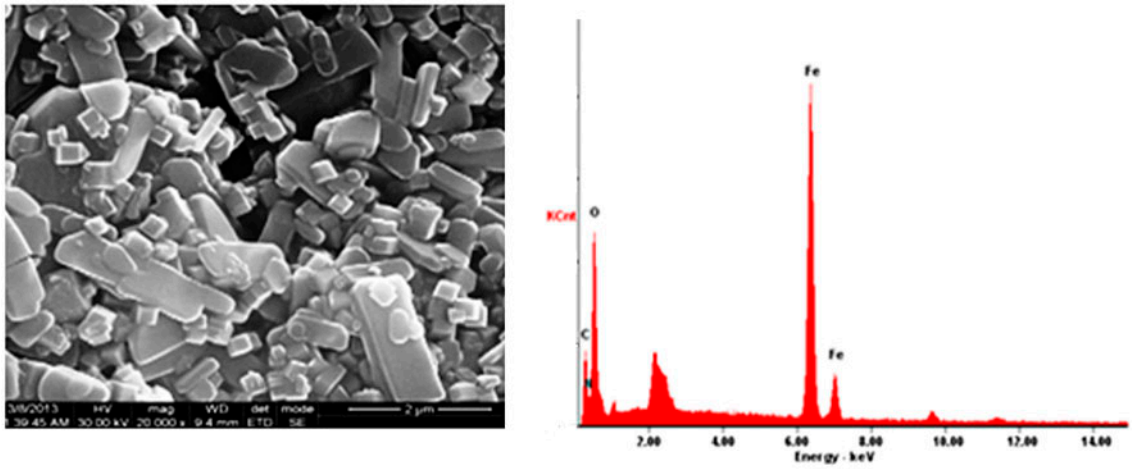

Fig. 3. SEM–EDAX photograph for iron Schiff base complex.

Table 1
Elemental analysis

	C%	H%	N%	S%	Fe%
Ligand (Schiff base)	61.99	5.5	12.16	14.98	–
Fe-Schiff complex	38.13	4.09	8.10	8.93	7.93

This indicates that the coordination of the ligand through the metal atoms via imine group [13]. The peaks at 420 and 467.12 cm^{-1} are due to the Fe–N stretching and Fe–O, respectively [13].

3.2. Degradation of refractory organics in wastewater

The wastewater was collected from a CETP, located in chemical manufacturing industrial cluster which engages in the production of aromatic compounds such as phenolic compounds and fused ring compounds. The characteristics of the initial wastewater are presented in Table 3. The wastewater was characterized for COD, 3,360 mg/L and BOD, 980 mg/L with biodegradable index of 0.29 and COD /TOC ratio of 2:8 and the components were in reduced state with ORP of −218 mv. The biodegradability index shows that the wastewater was a non-biodegradable in nature.

The Fenton oxidation of wastewater was carried out using difference conditions such as pH, time, temperature, dosage of H_2O_2, dosage of Fe-complex to arrive optimum conditions.

3.2.1. Optimization of conditions

The effect of time was carried out to determine the optimum reaction time. The study was carried out at different temperatures (30, 40, 50, 60, and 70°C), different pH (3.5, 4.5, 5.5, 7.0, and 8.5), different mass of the complex (0.05, 0.1, 0.15, 0.2, and 0.25 g), and different H_2O_2 concentrations (4, 8, 16, 24, and 32 mmol) and the reaction volume considered was 250 mL. It was observed that the percentage removal of COD increased up to 6 h and thereafter reaction reached the equilibrium. The initial linear increase in COD reduction may be attributed to the chemical oxidation of the dissolved organics in the wastewater with OH·. Thus, the optimized reaction time was 6 h. The poor removal of BOD compared to COD, may be attributed to

Table 2
FT-IR for Schiff base iron(II) complex

Compound	C = N cm^{-1}	N–H cm^{-1}	C = S cm^{-1}	O–H cm^{-1}	CLO_4 cm^{-1}	M–O cm^{-1}	M–N cm^{-1}
Ligand	1,620.11	3055.4	728	3,440	–	–	–
[Fe-Ligand]	1,614.77	3,063	724.31	3,543.21	1,230.5 1,085 973.1	467.12	420

Table 3
Initial parameters of wastewater

Parameter	Value
pH	8.2
Alkalinity	550
Total dissolved solids mg/L	860
ORP	−218
COD (mg/L)	3,360
BOD (mg/L)	980
TOC (mg/L)	1,200

the conversion of non-biodegradable organics to degradable organics in wastewater.

3.2.2. Optimization of pH

The solution pH is an important controlling parameter in the oxidation process. The reaction was carried out at different pH (3.5, 4.5, 5.5, 7.0, and 8.5) to determine the optimum pH. About 0.25 g of iron Schiff base complex and 4 mmol of H_2O_2 could cause the maximum reduction in COD (53%) at pH 7.0 in 6 h (Fig. 4(a)). The temperature of the reaction is maintained at 50˚C. Previous reports on Fenton oxidation process [14,15] concluded that Fenton oxidation process was efficient at pH 3.5, whereas the present investigation confirmed the accomplishment of Fenton reaction at neutral pH which is considered to be a major advantage. In conventional Fenton treatment, at pH greater than five the complexation of Fe^{2+} as [Fe (II) $(H_2O)_6]^{2+}$ was favored which reacted more slowly with H_2O_2 to form [Fe(II) (OH) $(H_2O)_5]^{2+}$ and thus producing less amount of hydroxyl radicals [1]. Because of the usage of Iron (II) as a complex the above said reaction is not possible, thus, it favors the oxidation process up to pH 7.0.

3.2.3. Effect of temperature

Temperature is considered to be an important variable for the oxidation process. The effect of temperature on the oxidation of dissolved organics in wastewater was carried out at different temperatures (30, 40, 50, 60, and 70˚C) with iron Schiff base complex, 0.25 g; H_2O_2, 4 mmol; pH 7.0 and hydraulic retention time, 6 h. The COD destruction from the wastewater increased with increase in temperature up to 60˚C (Fig. 4(c)). The activation energy for the oxidation of COD was 8.13 kJ/mol.

3.2.4. Effect of mass of the iron complex

The effect of mass of Fe(II) Schiff base complex on the oxidation of COD was determined with different

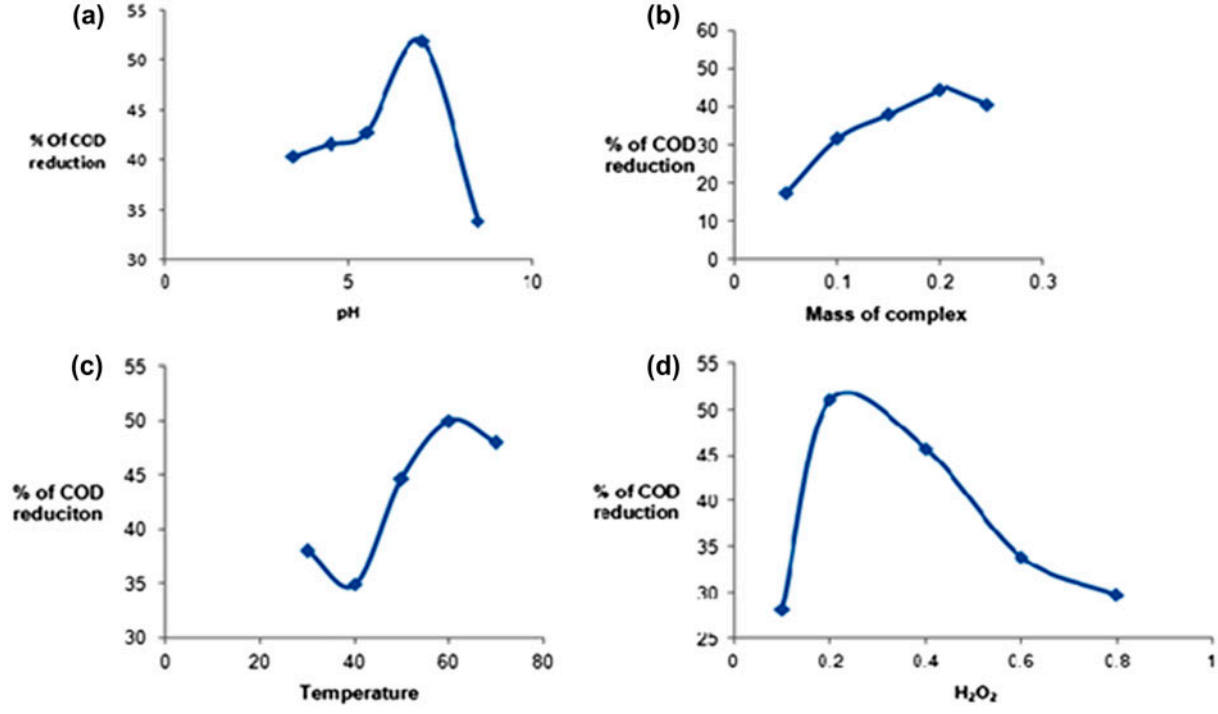

Fig. 4. Influence of (a) pH, (b) mass of the complex, (c) temperature, and (d) H_2O_2 dosage on the reduction of COD.

mass of the complex such as 0.05, 0.1, 0.15, 0.2, and 0.25 g and other conditions maintained were H_2O_2, 4 mol, hydraulic retention time, 6 h; pH 7.0 and temperature, 60°C. The oxidation of organics in wastewater increased with increase in mass of Fe(II) Schiff base complex. The maximum reduction in COD was obtained at dosage of 0.2 g (Fig. 4(b)).

3.2.5. Effect of H_2O_2

The effect of hydrogen peroxide on the oxidation of dissolved organics in wastewater was determined by varying the concentration of hydrogen peroxide (4, 8, 16, 24, and 32 mmol) while maintaining the conditions as mass of complex, 0.25 g; pH 7.0; temperature, 60°C; and hydraulic retention time, 6 h. Thus, the ratio of [iron–Schiff base]: [H_2O_2] maintained was 1:0.5, 1:1, 1:2, 1:3, and 1:4. The COD, BOD, and TOC removal increased with increase in hydrogen peroxide concentration up to 8 mmol and decreased thereafter (Fig. 4(d)). Thus, the optimum ratio observed was 1:1.

3.2.6. Oxidation of organics in wastewater at optimized conditions

The oxidation of organics in wastewater at the optimized conditions was carried out at temperature, 60°C; pH 7.0; mass of the complex, 0.2 g; H_2O_2, 8 mmol, hydraulic retention time, 6 h; and volume of wastewater, 250 mL. The COD of the wastewater was reduced from 3,360 to 1,200 mg/L at the optimum conditions and BOD/COD was increased to 0.44 and COD/TOC was increased to 3.6. Thus, the biodegradability index indicates that the wastewater was turned to be biodegradable in nature. The characteristics of wastewater after treatment were COD, 1,200 mg/L; BOD, 524 mg/L; TOC, 330 mg/L.

3.3. Kinetic studies for the Fenton oxidation reactions

The Fenton oxidation reaction kinetics was well fitted with second-order rate kinetics with regression coefficient of 0.96 at optimized conditions (Fig. 5). The second-order mathematical expression used for validating the kinetics is denoted as Eq. (3)

$$1/[A]t = 1[A]0 + kt \quad (3)$$

where [A]0—COD of wastewater at time, t=0, [A]t—COD of wastewater at any time, (t), t—time, in hours, k—rate constant, L mg^{-1} min^{-1}.

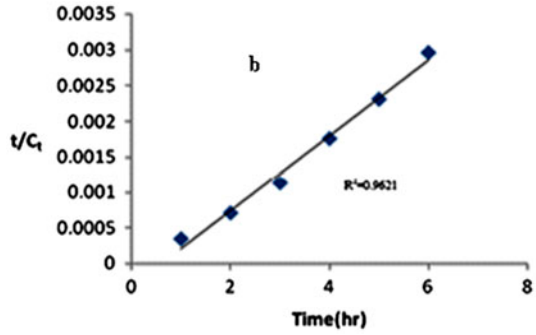

Fig. 5. Plot of second-order kinetic model at optimized conditions.

Thus, it indicates that the concentration of the iron–Schiff base complex as well as H_2O_2 determination rate.

The rate constants determined at different temperatures were used to calculate the activation energy of reaction as shown in Eq. (4):

$$\ln k_e = E_a/RT + \ln A \quad (4)$$

where E_a—Arrhenius activation energy of oxidation process, indicating the minimum energy that reactants must possess for the reaction to proceed, A—Arrhenius factor, R—gas constant (8.314 J mol^{-1} k^{-1}), k_e—rate constant, and T—temperature.

The slope of the straight line was made by plotting ln k_e vs. $1/T$ (Fig. 6) and calculated by linear fitting to obtain the apparent activation energy. The activation energy for the reaction oxidation process was 8.13 kJ mol^{-1}.

3.4. Analysis of thermodynamic parameters

The thermodynamic parameters such as Gibbs free energy (ΔG), change in enthalpy (ΔH), and change in entropy (ΔS) were calculated for the oxidation process.

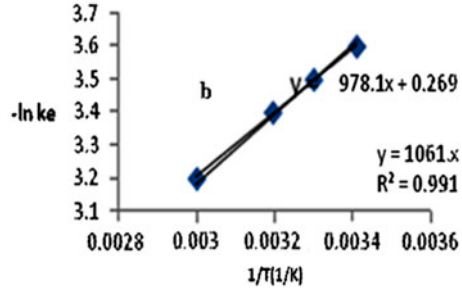

Fig. 6. Determination of E_a at optimized condition reaction.

From the plot of ln (K_{eq}) against $1/T$, the ΔS and ΔH-values were calculated using Vant–Hoff rate equation (Eq. 5)

$$\ln k_{eq} = \Delta S/R - \Delta H/RT \quad (5)$$

where k_{eq}—reaction equilibrium constant, the ΔH and ΔS values were found to be 21.98 and 73.31 J mol^{-1} K^{-1}.

The positive value of ΔH indicates that the oxidation process was an endothermic process and the positive value of ΔS indicates the random orientation of the converted products at the solid–solution interface.

The free energy of oxidation reaction was related with the ΔH and ΔS by the mathematical expression.

$$\Delta G = \Delta H - T\Delta S \quad (6)$$

The ΔG was calculated as −2.43 kJ mol^{-1}. The negative sign of ΔG value indicates the spontaneity of the oxidation process of wastewater.

3.5. ^{13}C NMR

3.5.1. Initial wastewater

Fig. 7(a) shows chemical shift at δ 115–140 ppm, refers to the aromatic compounds present in the wastewater. Depending upon the substitution, the chemical shift of the aromatic compound varied from δ 128.5 to 135 ppm. The shift in the range δ 160–180 ppm refers to the carboxylic acid derivatives. The chemical shift of 17.5 ppm refers to the methyl group substituted to the aromatic ring and the chemical shift present at δ 39.5–40.5 ppm is due to the solvent CD_3SOCD_3(DMSO-d6).

3.5.2. ^{13}C-NMR treated water

Most of the chemical shifts occurred in the range of δ 120–140 ppm in the treated water (Fig. 7(b)) and also there is a change in the chemical shift of methyl group which is attached to the aromatic ring. The new chemical shift formed at δ 50 ppm may be due to the methyl group attached to the OH group which may be formed due to the breakage of the phenolic groups present in the initial wastewater.

3.6. ^{1}H-NMR

3.6.1. Initial wastewater

The chemical shift present from δ 6.5 to 8 ppm refers to the aromatic rings. The fused benzene rings referred by the chemical shift at δ 7.7–7.8 ppm in Fig. 7(c), whereas mono-substituted aromatic confirm at δ 7.44 ppm. The chemical shift from δ 6.6 to 7 ppm corresponds to change in the mono-substituted aromatic rings due to the presence of –OH (or) –NH_2 groups. The chemical shift present at δ 4.8 ppm can be attributed to phenolic OH group. The aryl amines

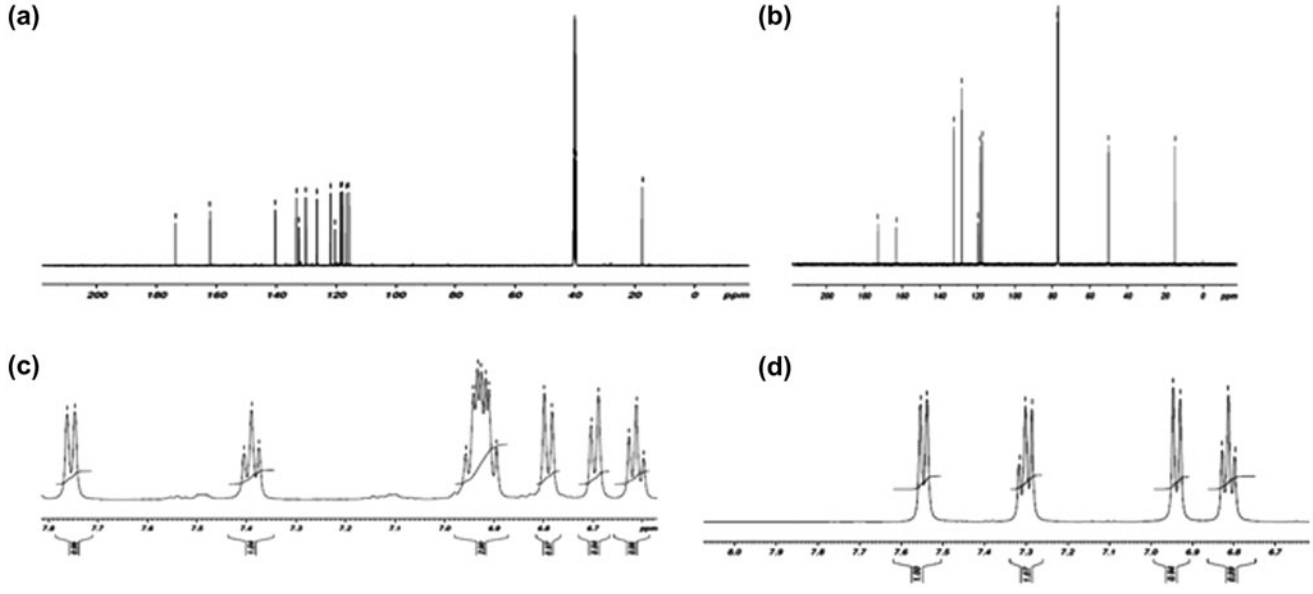

Fig. 7. (a) C13 NMR for initial waste water, (b) C13 NMR for treated wastewater, (c) H1 NMR 477 for initial wastewater, and (d) H1 NMR for treated wastewater.

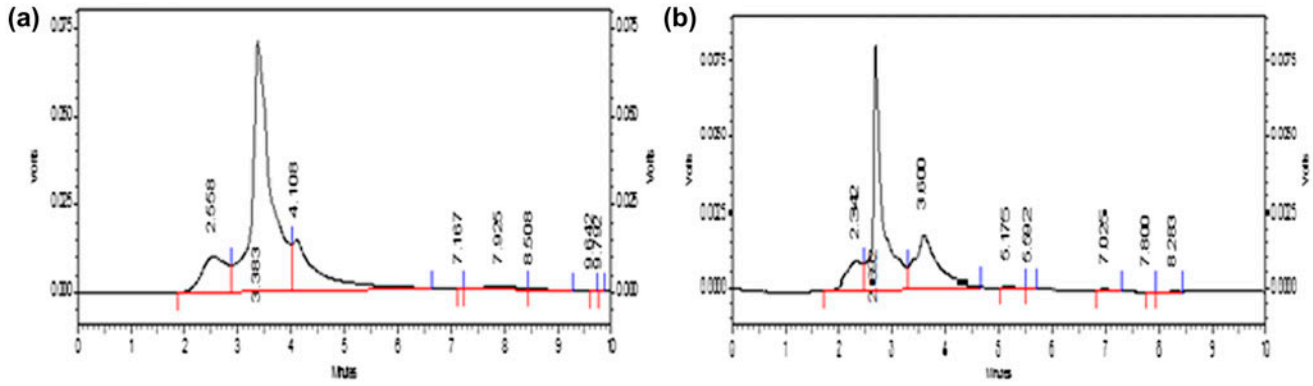

Fig. 8. (a) HPLC for initial wastewater and (b) HPLC for treated wastewater.

exhibit at δ 3.8–4 ppm and the methyl groups attached to aromatic ring is indicated by the chemical shift at δ 2.3 ppm.

3.6.2. Treated wastewater

^{1}H-NMR of the treated wastewater clearly demonstrates that there is a change in the chemical shift of aromatic rings in the region of δ 7.3–7.6 ppm. Moreover, there is a loss of chemical shift in the range of substituted aromatic ring in the region of δ 6.6–7 ppm (Fig. 7(d)). The chemical shift due to phenolic –OH was absent in the treated wastewater and moreover there is a change in the aryl amines chemical shift at δ 3.8–4 ppm.

3.7. HPLC

Initial wastewater and treated wastewater were further analyzed in reversed phase HPLC using acetonitirile as the mobile phase.

The wastewater before oxidation has the evidence for organic compounds corresponding to retention time at 2.558, 3.383 (the major compounds), and 4.108 min as shown in Fig. 8(a). In Fig. 8(b), HPLC spectrum showed these compounds were eliminated during oxidation with Fe(II)–Schiffs base complex and the new compounds were formed with retention times of 2.342, 2.692, and 3.6 min. This is well supported by the UV–Visible spectroscopy.

3.8. Fluorescence for initial and final samples

The excitation spectra of initial wastewater displayed the maximum excitation wavelength at λ 328 nm. Upon excitation at 328 nm, weak emission band at 472 nm (Fig. 9(a)) is observed. But the treated water showed the maximum excitation wavelength at λ 306 nm and its corresponding emission at λ 451 nm (Fig. 9(b)). The instrumentation evidences for the degraded fragmented products confirm the degradation of phenolic and fused aromatic ring compounds in wastewater.

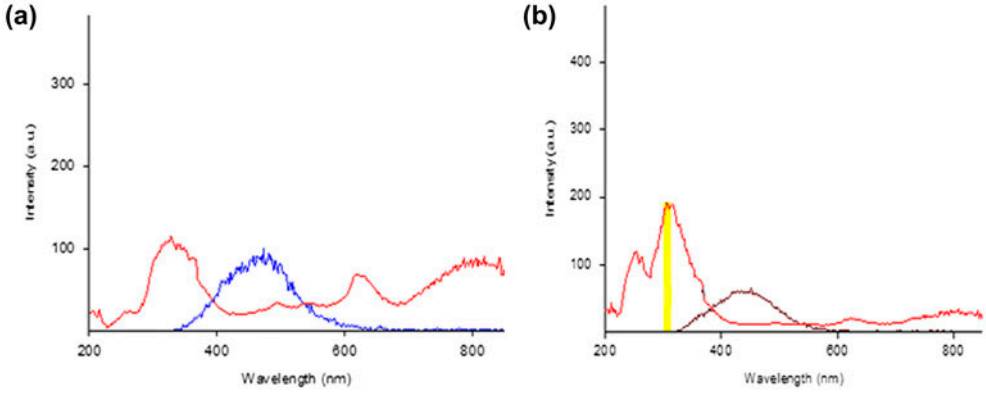

Fig. 9. (a) Fluorescence spectrum for initial wastewater and (b) Fluorescence spectrum for treated wastewater.

4. Conclusion

Synthesis, characterization, and application of Fe–Schiff base complex in wastewater treatment has been detailed in this manuscript. The Fe–Schiff base complex with H_2O_2 was used in the oxidation process of chemical industry wastewater at pH 7.0 while conventional Fenton process is used only at acidic pH 3.5. The reduction of COD was observed from 3,360 to 1,200 mg/L (64% reduction) at optimized conditions. The degradation studies were confirmed with the instrumental evidences such as ^{13}C-NMR, ^{1}H-NMR, HPLC, and fluorescence spectroscopy. This study concluded that the inorganic iron Schiff base complex can be used as an alternative to Fenton's reagent at neutral pH.

Acknowledgments

The authors are thankful to the council of scientific and industrial research (CSIR) and the Central Leather Research Institute, India, for giving financial support under STRAIT CSC 0201 for conducting the experiments.

References

[1] S. Karthikeyan, M. Ezhil Priya, R. Boopathy, M. Velan, A.B. Mandal, G. Sekaran, Heterocatalytic Fenton oxidation process for the treatment of tannery effluent: Kinetic and thermodynamic studies, Environ. Sci. Pollut. Res. Int. 19 (2012) 1828–1840.

[2] I.P. Ivanova, S.V. Trofimova, I.M. Piskarev, N.A. Aristova, O.E. Burhina, O.O. Soshnikova, Mechanism of chemiluminescence in Fenton reaction, J. Biophys. Chem. 3 (2012) 88–100.

[3] E. Chamarro, A. Marco, S. Esplugas, Use of Fenton reagent to improve organic chemical biodegradability, Water Res. 35 (2001) 1047–1051.

[4] J. Herney-Ramirez, M.A. Vicente, L.M. Madeira, Heterogeneous photo-Fenton oxidation with pillared clay-based catalysts for wastewater treatment: A review, Appl. Catal., B 98 (2010) 10–26.

[5] A.K. Patra, A. Dutta, A. Bhaumik, Mesoporus core–shell Fenton nanocatalyst: A mils, operationally simple approach to the synthesis of Adipic acid, Chem. Eur. J. 19 (2013) 12388–12395.

[6] S.H. Bossmann, E. Oliveros, S. Gob, M. Kantor, A. Goppert, L. Lei, P.L. Yue, A.M. Braun, Degradation of polyvinyl alcohol (PVA) by homogeneous and heterogeneous photocatalysis applied to the photochemically enhanced Fenton reaction, Water Sci. Technol. 44 (2001) 257–262.

[7] J. Feng, X. Hu, P.L. Yue, Discoloration and mineralization of Orange II by using a bentonite clay-based Fe nanocomposite film as a heterogeneous photo-Fenton catalyst, Water Res. 39 (2005) 89–96.

[8] S. Karthikeyan, C.J. Magthalin, A.B. Mandal, G. Sekaran, Controlled synthesis and characterization of electron rich iron (III) oxide doped nanoporous activated carbon for the catalytic oxidation of aqueous ortho phenylene diamine, RSC Adv. 4 (2014) 19183–19195.

[9] S. Karthikeyan, A. Titus, A. Gnanamani, A.B. Mandal, G. Sekaran, Treatment of textile wastewater by homogeneous and heterogeneous Fenton oxidation processes, Desalination 281 (2011) 438–445.

[10] H.N. Aliyu, H. Adamu, Synthesis and characterization of N-(I-morpholinobenzyl) semicarbazide manganese (II) and iron (II) complexes, Bayero J. Pure Appl. Sci. 2 (2009) 143–148.

[11] N. Kumar, P. Sharma, A. Pareek, A.V.G.S. Prasad, Synthesis and characterization of some new shiff bases, Int. J. Chem. Phys. Sci. 4 (2013) 12–18.

[12] CPCB, Inventorisation of Hazardous Waste Generation in Five Districts (Ahmedabad, Vadodara, Bharuch, Surat and Valsad) of Gujarat, Central Pollution Control Board (Ministry of Environment & Forests, Government of India), 1996, ISBN 8186396632.

[13] B. Rizwana, S.S. Lakshmi, Synthesis, characterisation and antimicrobial studies of Zn(II), Ni(II) and Cu(II) complexes of a schiff base derived from o-vanillin and n-allyl thiourea, Int. J. ChemTech Res. 4 (2012) 464–473.

[14] K. Chitra, K.S.B. Kameswari, L.V. Devi, S. Porselvam, J.R. Rao, Combined advanced oxidation processes and aerobic biological treatment for synthetic fatliquor used in tanneries, Ind. Eng. Chem. Res. 51 (2012) 16171–16181.

[15] M.L. Kremer, Mechanism of the Fenton reaction. Evidence for a new intermediate, Phys. Chem. Chem. Phys. 1 (1999) 3595–3605.